Available online at www.sciencedirect.com
ScienceDirect
Journal of Power Sources 174 (2007) 352–358
JOURNAL OF POWER SOURCES
www.elsevier.com/locate/jpowsour

Analysis of SEI formed with cyano-containing imidazolium-based ionic liquid electrolyte in lithium secondary batteries

Liwei Zhao [a,*], Jun-ichi Yamaki [a], Minato Egashira [b]

[a] *Institute for Materials Chemistry and Engineering, Kyushu University, 6-1 Kasuga-Koen, Kasuga, Fukuoka 816-8580, Japan*
[b] *Department of Applied Chemistry and Chemical Engineering, Faculty of Engineering, Yamaguchi University, 2-16-1, Yamaguchi 755-8611, Japan*

Available online 28 June 2007

Abstract

Two kinds of cyano-containing imidazolium-based ionic liquid, 1-cyanopropyl-3-methylimidazolium-bis(trifluoromethanesulfonyl)imide (CpMI-TFSI) and 1-cyanomethyl-3-methylimidazolium-bis(trifluoromethanesulfonyl)imide (CmMI-TFSI), each of which contained 20 wt% dissolved LiTFSI, were used as electrolytes for lithium secondary batteries. Compared with 1-ethyl-3-methylimidazolium-bis(trifluoromethanesulfonyl)imide (EMI-TFSI) electrolyte, a reversible lithium deposition/dissolution on a stainless-steel working electrode was observed during CV measurements in these cyano-containing electrolytes, which indicated that a passivation layer (solid electrolyte interphase, SEI) was formed during potential scanning. The morphology of the working electrode with each electrolyte system was studied by SEM. Different dentrite forms were found on the electrodes with each electrolyte. The SEI that formed in CpMI-TFSI electrolyte showed the best passivating effect, while the deposited film formed in EMI-TFSI electrolyte showed no passivating effect. The chemical characteristics of the deposited films on the working electrodes were compared by XPS measurements. A component with a cyano group was found in SEIs in CpMI-TFSI and CmMI-TFSI electrolytes. The introduction of a cyano functional group suppressed the decomposition of electrolyte and improved the cathodic stability of the imidazolium-based ionic liquid. The reduction reaction route of imidazolium-based ionic liquid was considered to be different depending on whether or not the molecular structure contained a cyano functional group.

Keywords: Lithium secondary batteries; Ionic liquid electrolyte; Solid electrolyte interphase (SEI); XPS; SEM

1. Introduction

Lithium secondary batteries have become an important energy storage device for portable electronic instruments and electric vehicles. Among the many kinds of negative electrode, lithium metal electrode is of special interest to battery researchers due to it higher theoretical energy density. However, during practical cycling, the repetitive deposition and dissolution of lithium results in a dentritic morphology on the electrode surface, which can cause safety hazards and drastically reduce the cycle life [1,2]. The growth of dendrites can create a short circuit in the cell, which can cause significant local heating and often lead to a fire and explosion. The use of volatile and flammable organic solvents can further worsen the safety hazard associated with batteries.

To promote the safety and performance of batteries, many different ionic liquids have been investigated for use as solvents in lithium battery electrolyte due to their unique electrochemical and physical properties. The favorable properties include negligible flammability, nonvolatility, high ionic conductivity, wide electrochemical window and low toxicity, which promise a safer electrolyte. Most of the ionic liquids that have been reported to date contain large organic cations with a delocalized charge, such as quaternary ammonium [3–5], pyrrolidinium [6], triazolium [7], phosphornium [8], piperidinium [9] and particularly imidazolium [10–12], combined with a variety of anions. With regard to the anion, the bis(trifluoromethanesulfone)imide ($TFSI^-$) anion has been widely studied and recently applied due to its particular ability to lower the melting point of ionic solvents [6,13].

Compared with other kinds of ionic liquid, imidazolium-based ionic liquid has received much attention because of its high conductivity, low viscosity and low melting point. Among them, 1-ethyl-3-methylimidazolium-bis(trifluoromethanesulfonyl)imide (EMI-TFSI) has been most widely studied [14,15].

* Corresponding author. Tel.: +81 92 583 7657; fax: +81 92 573 7791.
E-mail address: zhaolw@cm.kyushu-u.ac.jp (L. Zhao).

0378-7753/$ – see front matter © 2007 Elsevier B.V. All rights reserved.
doi:10.1016/j.jpowsour.2007.06.131

However, the cathodic stability of imidazolium-based ionic liquids is not sufficient for the reversible charge–discharge of negative electrodes. To prevent the further decomposition of electrolyte on the surface of the lithium electrode, the formation of a solid electrolyte interphase (SEI) is assumed to be a key factor in the properties of lithium batteries. Several additives, such as H_2O [16], HCl [17], and organic solvent [18,19], have been used to accelerate SEI formation. Unfortunately, some of these additives poison battery performance. Therefore, an ionic liquid capable of providing an SEI on a lithium surface should be an ideal solvent for electrolyte.

In the present study, two kinds of air and moisture-stable cyano-containing imidazolium-based ionic liquid, 1-cyanopropyl-3-methylimidazolium-bis(trifluoromethanesulfonyl)-imide (CpMI-TFSI) and 1-cyanomethyl-3-methylimidazolium-bis(trifluoromethanesulfonyl)imide (CmMI-TFSI) were used as electrolytes, and each contained 20 wt% dissolved LiTFSI. Lithium electrodeposition/dissolution was performed on a stainless-steel electrode. The formation of an SEI was investigated by CV, XPS, and SEM measurements. The effect of the structural formula of the ionic liquid on the electro-chemical properties and SEI formation is discussed. For comparison, EMI-TFSI with 20 wt% dissolved LiTFSI was also used as an electrolyte in this study.

2. Experimental

Two kinds of cyano-containing imidazolium-based ionic liquid, CpMI-TFSI and CmMI-TFSI (The Nippon Synthetic Chemical Industry Co., Japan) were used as electrolyte solvents. The structural formulas of the two cations in this study are shown in Fig. 1. The electrolyte was prepared by dissolving 20 wt% LiTFSI in the test ionic liquid. For comparison, EMI-TFSI, which contained 20 wt% dissolved LiTFSI, was also used as an electrolyte. The structural formula of EMI cation is also shown in Fig. 1. Hereafter, the three kinds of electrolytes, CpMI-TFSI with 20 wt% dissolved LiTFSI, CmMI-TFSI with 20 wt% dissolved LiTFSI, and EMI-TFSI with 20 wt% dissolved LiTFSI are referred to as CpMI-TFSI electrolyte, CmMI-TFSI electrolyte, and EMI-TFSI electrolyte,

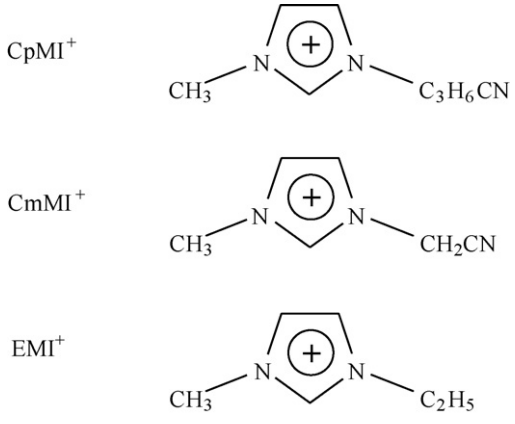

Fig. 1. Structural formulas of cations for imidazolium-based ionic liquids in the present study.

respectively. The viscosity and conductivity of the ionic liquids and electrolytes are described in Ref. [20].

Electrochemical lithium deposition/dissolution in electrolytes was studied in a two-electrode half-cell. The electrochemical cell consisted of a stainless-steel foil working electrode, a polypropylene separator (Celgard 3501) and a lithium-foil counter electrode. All cells were assembled in an argon-filled glove box.

Electrochemical pretreatment was performed by a CV experiment in the range of −0.5 to 2.5 V versus Li/Li^+ at a scan rate of 0.5 mV/s unless stated otherwise, with an equilibration time of 60 s before the first CV scan. All electrochemical pretreatments were carried out at 25 °C.

After CV measurement, the pre-cycled cells were dismantled in an Ar-filled glove box. The stainless-steel electrode was rinsed and soaked in DMC for 1 h and vacuum-dried at room temperature for 2 h. Most of the low-molecular weight components were dissolved away from the SEI in the rinsing step and evacuated during vacuum-drying.

The surface of the electrodeposited lithium was analyzed by XPS (JPS-9010MC/IV, JEOL) under ultrahigh-vacuum conditions (less than 5×10^{-7} Pa). The X-ray source was a monochromatic Mg Kα radiation (1253.6 eV). High-resolution spectra were summed over 10 scans with pass-energies of 10 and 30 eV. A portable vacuum carrier was used to transfer the sample from the glove box to the XPS sample chamber.

The surface morphology of the electrodeposited lithium was observed with a scanning electron microscope combined with an energy dispersive spectroscope (SEM-EDS, JSM-6060 LA/VI, JEOL). The sample was treated in the same way as for the XPS analysis. The sample was transferred from the Ar-filled glove box to the SEM sample chamber using a portable vacuum carrier and was not exposed to air during transit.

3. Results and discussion

Since they are both imidazolium-based cations, $CpMI^+$ and $CmMI^+$ have structural formulas similar to that of EMI^+, as shown in Fig. 1. EMI-based ionic liquid has been reported to have poor cathodic stability and cannot form a passivation layer on deposited lithium. The introduction of a cyano group was suggested to be an effective way to improve the cathodic stability of ionic liquid [4]. Fig. 2 shows cyclic voltammograms of working electrodes in CpMI-TFSI and CmMI-TFSI electrolytes at 25 °C. For comparison, the cyclic voltammogram of a stainless-steel electrode in EMI-TFSI electrolyte is also shown. As expected, the EMI-TFSI system showed no anodic CV peak, but a much higher irreversible cathodic current started at higher potential than in the CpMI-TFSI and CmMI-TFSI systems, and this was attributed to the reduction decomposition of EMI-TFSI and/or the electrodeposition of lithium. In contrast, when CpMI-TFSI and CmMI-TFSI were used as electrolyte solvents, clear anodic CV peaks were obtained at about 0.25 V versus Li/Li^+, which could be attributed to the dissolution of electrodeposited lithium. Therefore, a reversible lithium deposition/dissolution couple was proposed in both electrolytes. This phenomenon indicated that passivation layers formed on the electrode sur-

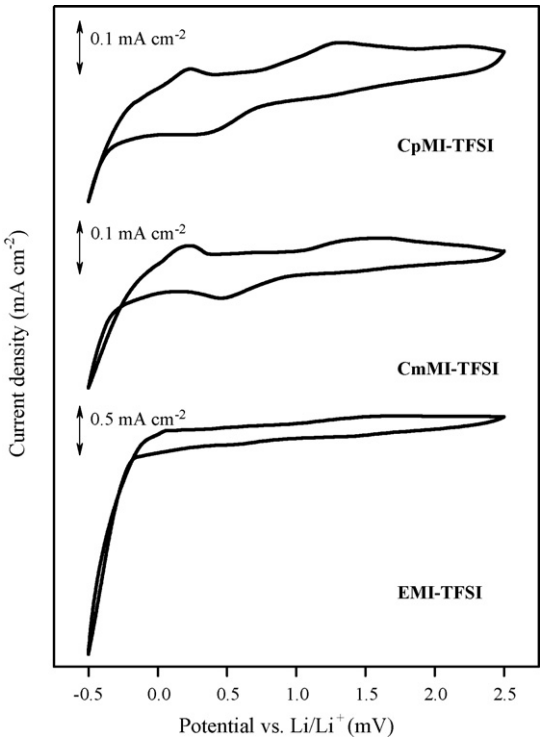

Fig. 2. Cyclic voltammograms for lithium deposition/dissolution on a stainless-steel electrode at 25 °C in CpMI-TFSI, CmMI-TFSI and EMI-TFSI electrolytes, respectively.

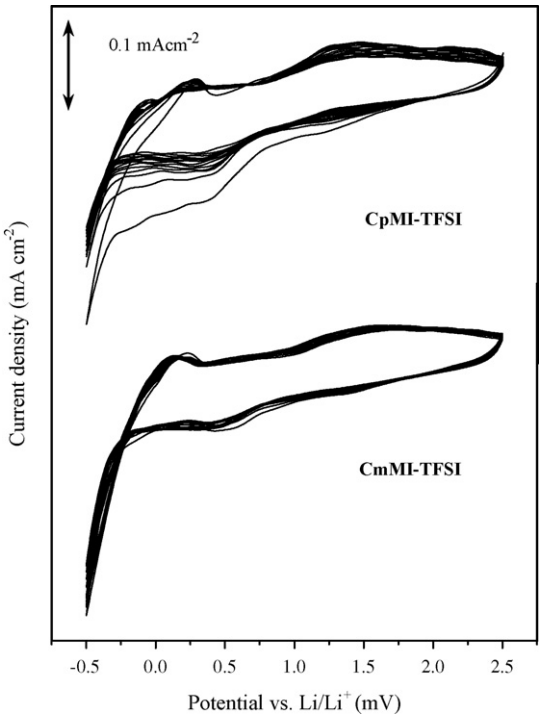

Fig. 3. Multiple cyclic voltammograms for lithium deposition/dissolution on stainless-steel electrode at 25 °C in CpMI-TFSI and CmMI-TFSI, respectively, for 20 CV cycles.

faces in CpMI-TFSI and CmMI-TFSI electrolytes. Considering that the structural formulas of $CpMI^+$ and $CmMI^+$ are similar to that of EMI^+, the introduction of a cyano group was believed to be key factor for the formation of an SEI on the electrode surface.

Compared to the reduction current density at −0.5 V, a much lower oxidation current density was obtained at +0.25 V in both CpMI-TFSI and CmMI-TFSI electrolytes. This indicates that the electrodeposition of lithium contributed only part of the reduction current. Another source of reduction current, indeed the main contributor, was considered to be the electro-reduction of electrolytes.

Although CpMI-TFSI and CmMI-TFSI showed cyclic voltammograms similar to each other in Fig. 2, the reduction current (mainly caused by electrolyte reduction) in CpMI-TFSI electrolyte was lower than that in CmMI-TFSI electrolyte. Thus, the reduction of electrolyte was serious in CmMI-TFSI electrolyte than in CpMI-TFSI electrolyte. Furthermore, a more efficient passivation film was obtained in CpMI-TFSI electrolyte than in CmMI-TFSI electrolyte. Fig. 3 shows the cyclic voltammograms of stainless-steel electrodes for 20 potential scan cycles in CpMI-TFSI and CmMI-TFSI electrolytes, respectively, at 25 °C. Compared with that in CmMI-TFSI electrolyte, the reduction current at −0.5 V decreased gradually with the cycle number in CpMI-TFSI electrolyte. These phenomena indicated that the SEIs formed in CpMI-TFSI and CmMI-TFSI electrolytes had different properties. The SEI in the former had better electrochemical characteristics than that in the latter, which meant it had a better passivating effect to protect the solvent molecules from further reduction decomposition.

To study the SEIs on electrodeposited lithium more clearly, the morphology of stainless-steel working electrodes was observed by SEM measurement after multiple CV scans stopped at a potential of 2.5 V. At this potential, electrochemically active lithium was dissolved from the working electrode, while only electrochemically isolated lithium (dead lithium) remained on the electrode. The dead lithium is electrochemically inactive but chemically active. The morphology of dead lithium should reveal the morphology of electrodeposited lithium. Fig. 4 shows SEM images of the surface of stainless-steel electrodes after multiple potential scanning in CpMI-TFSI, CmMI-TFSI, and EMI-TFSI electrolytes, respectively. In both CpMI-TFSI and CmMI-TFSI electrolytes, lithium dentrites were observed on the electrodes after 5 CV scans in the range of −0.5 to 2.5 V. The electrodeposited lithium showed different patterns in the two electrolytes. In CmMI-TFSI electrolyte, a kind of glossy and slim fiber-like lithium dentrite with a length of 2–3 μm was observed. In CpMI-TFSI electrolyte, the deposited lithium showed particle-like dentrites, sometimes mixed with lithium fibers. On the other hand, the distributions of dead lithium were also different in the two electrolytes. Fewer dead lithium remained on the electrode surface in CpMI-TFSI electrolyte than in the other electrolyte, which also suggested better lithium cycling efficiency in CpMI-TFSI electrolyte. This difference in morphology was thought to be caused by the different passivating effects of SEIs in CmMI-TFSI and CpMI-TFSI electrolytes. The growth of a fiber-like lithium dentrite was suppressed in CpMI-TFSI electrolyte due to the formation of an SEI with

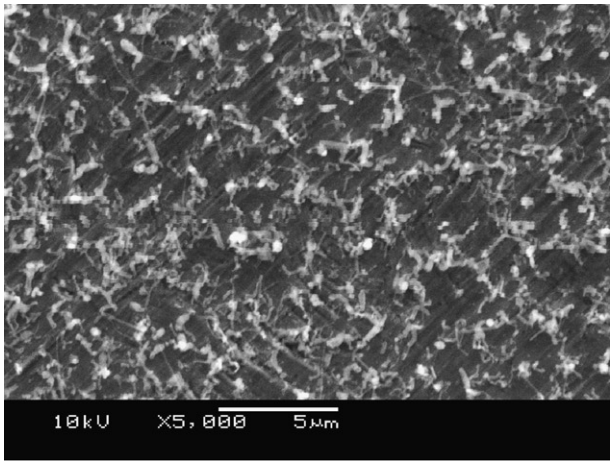

(a)

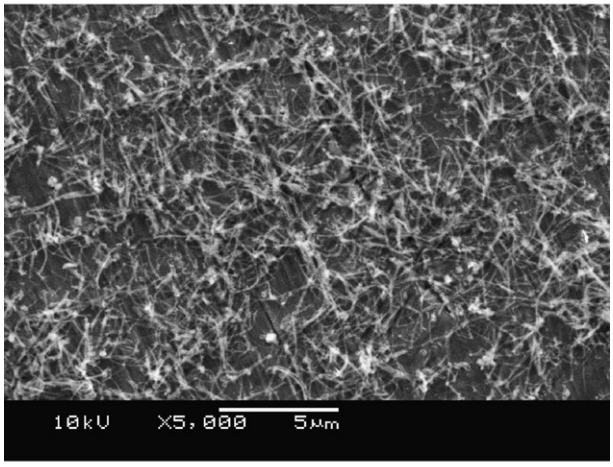

(b)

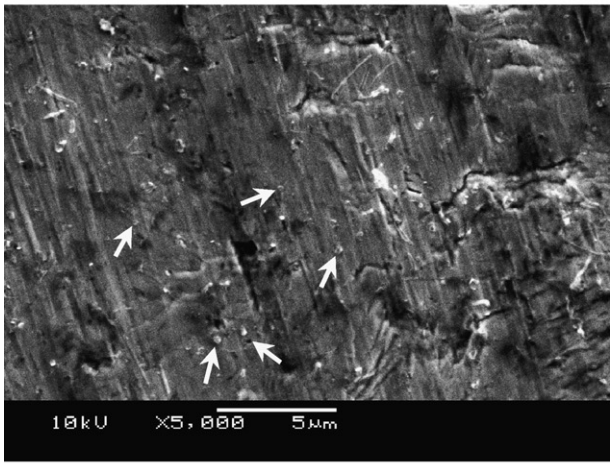

(c)

Fig. 4. SEM images of the stainless-steel electrode with (a) CpMI-TFSI electrolyte, (b) CmMI-TFSI electrolyte and (c) EMI-TFSI electrolyte after 5 CV scans in the range of +2.5 to −0.5 V vs. Li/Li^+.

a good passivating effect. Since the fiber-like lithium dentrite was easier to cut and thus become electrochemically inactive than the particle-like lithium dentrite [21], more dead lithium was obtained in CmMI-TFSI than in CpMI-TFSI electrolyte. In contrast, in EMI-TFSI electrolyte, no as-grown lithium dentrite was observed; only a rather thick deposited film was found on the electrode surface, with several stubs of broken dentrites immersed in it. This phenomenon suggested that very little lithium was deposited on the working electrode during CV scans, while the large reduction current at −0.5 V was due to the decomposition of EMI-TFSI electrolyte. Furthermore, the decomposition of EMI-TFSI caused a film deposited on the electrode surface, but the film did not contribute to the passivating effect of the seldom-deposited lithium. With the dissolution of deposited lithium during the CV scan, the lithium dentrite broke and generated dead lithium, which was chemically active and reacted with electrolyte. Finally, only several stubs of broken dentrite were left on the stainless-steel electrode.

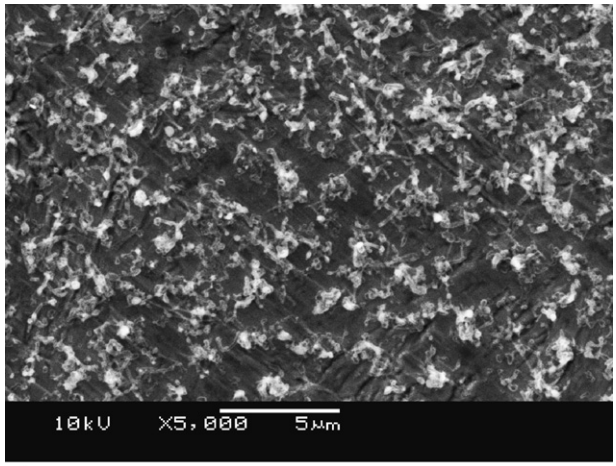

(a)

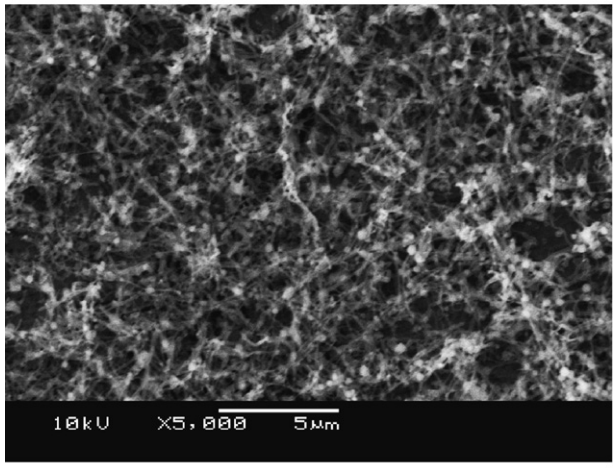

(b)

Fig. 5. SEM images of the stainless-steel electrode with (a) CpMI-TFSI electrolyte and (b) CmMI-TFSI electrolyte after 20 CV scans in the range of +2.5 to −0.5 V vs. Li/Li^+.

The growth of lithium dentrites with the CV scan number was clarified by comparing the SEM images obtained after 5 and 20 CV scans. Fig. 5 shows SEM images of the working electrodes after 20 CV scans in CpMI-TFSI and CmMI-TFSI electrolytes, respectively. The different lithium patterns in the two kinds of electrolytes persisted and became clearer. The amount of lithium on the electrodes increased because dead lithium accumulated during cycling. For CpMI-TFSI elec-

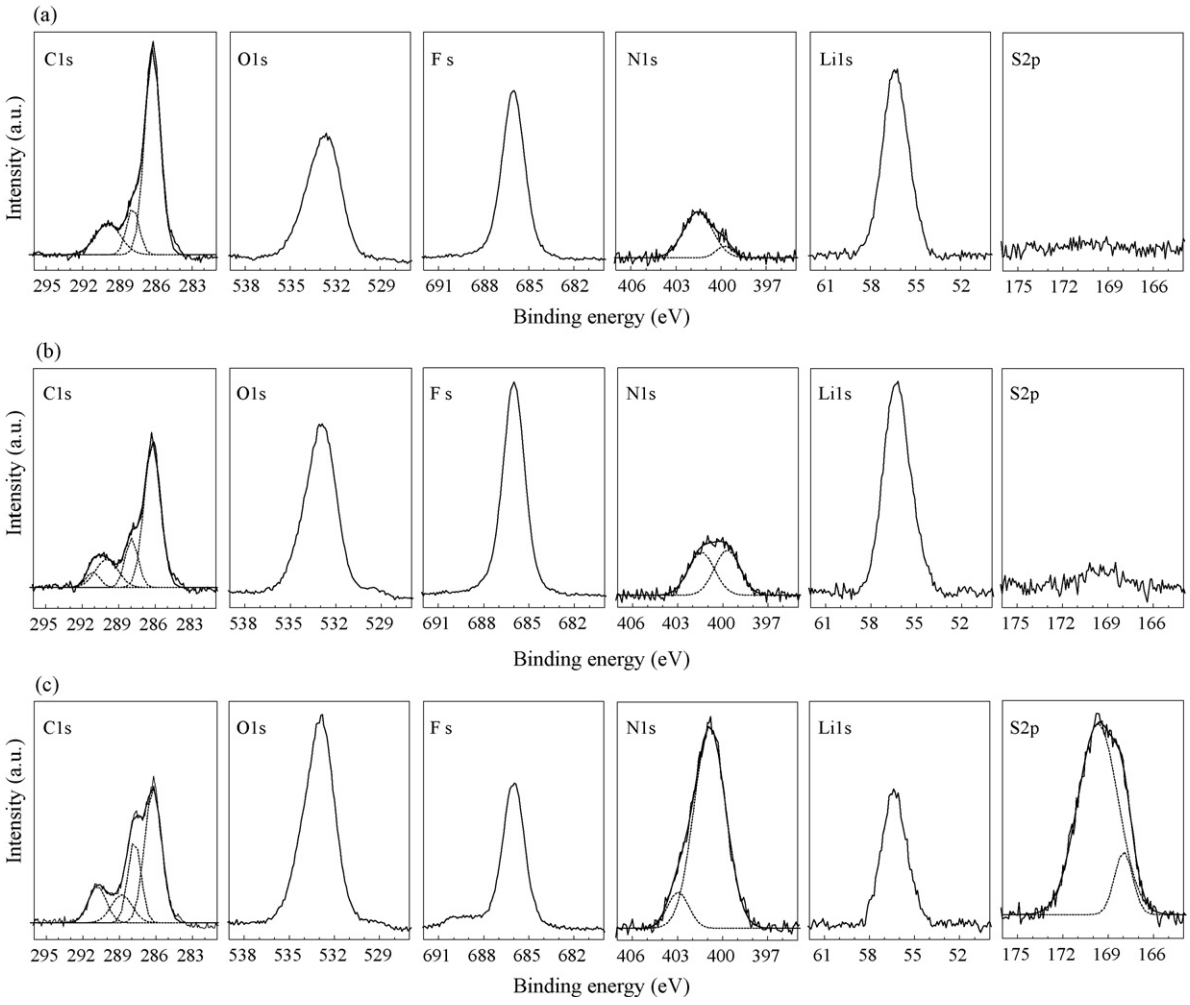

Fig. 6. XPS spectra of the stainless steel electrode with (a) CpMI-TFSI electrolyte, (b) CmMI-TFSI electrolyte and (c) EMI-TFSI electrolyte after 5 CV scans between +2.5 and −0.5 V vs. Li/Li^+.

trolyte, the growth of lithium dentrite caused larger lithium grains, and the density of lithium grains on the electrode also increased. In the case of CmMI-TFSI electrolyte, in addition to the thicker electrodeposited lithium, some particles appeared on the lithium dentrites. From EDS images, the particle showed higher fractions of carbon and oxygen compared with lithium fiber. Therefore, the particle was believed to have a thicker SEI layer than the lithium fiber.

Chemical characterization of the lithium-electrodeposited stainless-steel electrode was carried out with XPS. Fig. 6 shows the XPS spectra of C 1s, O 1s, N 1s, F 1s, Li 1s, and S 2p for the stainless-steel electrodes in the three kinds of electrolytes after 5 CV scans. In summary, the formation of deposited films on the electrode surface was observed in the electrochemical systems with three kinds of electrolytes, respectively. LiF was found to be an important component in all of the deposited films, and showed a peak at 56.3 eV in the Li 1s spectra and a peak at 686.0 eV in the F 1s spectra.

In comparing the XPS spectra, the most obvious difference between EMI-TFSI electrolyte and both the CpMI-TFSI and CmMI-TFSI electrolytes was noted in S 2p and N 1s spectra. In EMI-TFSI electrolyte, the S 2p signal showed a rather high intensity, while almost no relative peak was found in the spectra of the CpMI-TFSI and CmMI-TFSI systems. If we consider that $TFSI^-$ is the only source of elemental sulphur, the serious decomposition of $TFSI^-$ was thought to occur in EMI-TFSI electrolyte. In contrast, no significant decomposition of $TFSI^-$ was detected in CpMI-TFSI and CmMI-TFSI electrolytes. This supposition was confirmed by the strong N 1s signal in the spectra of EMI-TFSI electrolyte. The serious decomposition of $TFSI^-$ was reflected by a poor passivating effect of the reduction product of the EMI-TFSI electrolyte.

In addition to the S 2p and N 1s spectra, the C 1s spectra also showed a clear difference between the deposited film in EMI-TFSI electrolyte and the SEIs formed in CpMI-TFSI and CmMI-TFSI electrolytes. The C 1s peak at 287.9 eV was found in all three kinds of electrolyte. Moreover, with an increase in the duration of rinsing with DMC, the intensity of this peak gradually decreased. Therefore the C 1s peak at 287.9 eV was assigned to the C atoms in the imidazole ring. Another C 1s peak at 286.2 eV was also seen in all three kinds of deposited films, and this was attributed to hydrocarbon [22]. Although

the peak-positions were same, the intensity ratio of the peak at 286.2 eV to that at 287.9 eV was much lower in EMI-TFSI electrolyte than in the other two electrolytes. This means that the hydrocarbon fraction of the deposited film in EMI-TFSI was lower than those in the other two electrolytes, which could contribute to the poor passivating effect of the deposited film. This phenomenon was believed to be caused by a different reduction route for molecules in the electrolyte. For EMI-TFSI, no ring-open reduction reaction occurred, and the component with an imidazole ring showed a high fraction in the reduction product. For CpMI-TFSI and CmMI-TFSI, due to the existence of a cyano functional group, the imidazole ring was opened during electrochemical reduction. On the other hand, a C 1s peak at 290.0 eV was found in the deposited films in CpMI-TFSI and CmMI-TFSI electrolytes. This was believed to be due to a cyano functional group. The peak at 289 eV in C1s spectra of EMI-TFSI could be assigned to a C–F bond [23] caused by the reduction of LiTFSI [24].

In comparing the SEI formed in CpMI-TFSI electrolyte with that formed in CmMI-TFSI electrolyte, there are three notable differences. First, the intensity ratio of the peak at 286.2 eV to the peak at 287.9 eV in C 1s spectra in CpMI-TFSI electrolyte was obviously higher than that in CmMI-TFSI electrolyte, and this was believed to be partially caused by the long hydrocarbon chain in the molecular structure of CpMI-TFSI. This should at least partially explain the better passivating effect of the SEI formed in CpMI-TFSI electrolyte. Second, a peak at 291 eV was found in the C 1s spectrum of CmMI-TFSI electrolyte, which was also found in the C 1s spectrum of EMI-TFSI electrolyte but not in the spectrum of CpMI-TFSI electrolyte. Third, a distinguishable S 2p signal was obtained in CmMI-TFSI electrolyte, together with a much higher N 1s peak at 399.7 eV compared with the results in CpMI-TFSI electrolyte. The latter two points indicated slight reduction decomposition of $TFSI^-$ in CmMI-TFSI electrolyte, while no similar evidence was found in CpMI-TFSI electrolyte. The above three points were thought to cause the different passivating effects of the SEIs formed in CpMI-TFSI and CmMI-TFSI electrolytes.

4. Conclusion

In this study, two kinds of cyano-containing imidazolium-based ionic liquid, CpMI-TFSI and CmMI-TFSI, each of which contained 20 wt% dissolved LiTFSI, were used as electrolytes for lithium secondary batteries. Compared with EMI-TFSI electrolyte, a reversible lithium deposition/dissolution on a stainless-steel electrode was found during CV measurements in these two kinds of cyano-containing electrolyte. This reversible lithium deposition/dissolution was still stable after 20 CV scans, which indicated that a passivation layer (SEI) was formed during potential scanning. The introduction of a cyano functional group was effective for improving the cathodic stability of the imidazolium-based ionic liquid. The morphology of the stainless-steel working electrode with each electrolyte system was studied by SEM. Different dentrite forms were found on the electrodes with each electrolyte. The SEI formed in CpMI-TFSI electrolyte showed the best passivating effect, while the deposited film formed in EMI-TFSI electrolyte showed no passivating effect on the electrodeposited lithium and on protecting the solvent molecules from further reduction. The chemical characteristics of the deposited films on the working electrodes were compared by XPS measurements. The fraction of hydrocarbon in the deposited film was improved with the introduction of a cyano functional group. The reduction reaction route of imidazolium-based ionic liquid was thought to be different depending on whether or not the molecular structure contained a cyano functional group. The existence of a cyano functional group accelerated the ring-open reduction reaction of imidazole ring. A component with a cyano group was found in SEIs in CpMI-TFSI and CmMI-TFSI electrolytes. In comparing the two kinds of cyano-containing electrolyte, a more efficient passivation film was obtained in CpMI-TFSI electrolyte than in CmMI-TFSI electrolyte. This difference was believed to be caused by the different lengths of the carbon chains in the structural formulas of the ionic liquids.

Acknowledgements

Part of this work was supported by The Nippon Synthetic Chemical Industry Co. and CREST of JST (Japan Science and Technology Corporation).

References

[1] E. Peled, J. Power Sources 9 (1983) 253–266.
[2] J. Yamaki, S. Tobishima, K. Hayashi, K. Saito, Y. Nemoto, M. Arakawa, J. Power Sources 74 (1998) 219–227.
[3] J. Sun, M. Forsyth, D.R. MacFarlane, J. Phys. Chem. B 102 (1998) 8858–8864.
[4] M. Egashira, S. Okada, J. Yamaki, D.A. Dri, F. Bonadies, B. Scrosati, J. Power Sources 138 (2004) 240–244.
[5] M. Egashira, M. Nakagawa, I. Watanabe, S. Okada, J. Yamaki, J. Power Sources 146 (2005) 685–688.
[6] D.R. MacFarlane, P. Meakin, J. Sun, N. Amini, M. Forsyth, J. Phys. Chem. B 103 (1999) 4164–4170.
[7] B. Vestergaard, N.J. Bjerum, I. Petrushina, H.A. Hjuler, R.W. Gerg, M. Begtrup, J. Electrochem. Soc. 140 (1993) 3108–3113.
[8] J.D. Holbery, K.R. Seddon, Clean Products Process. 1 (1999) 223–236.
[9] H. Sakaebe, H. Matsumoto, Electrochem. Commun. 5 (2003) 594–598.
[10] L.A. Blanchard, D. Hancu, E.J. Beckman, J.F. Brennecke, Nature 399 (1999) 28–29.
[11] K. Sekiguchi, M. Atobe, T. Fuchigami, J. Electroanal. Chem. 557 (2003) 1–7.
[12] Y.S. Fung, R.Q. Zhou, J. Power Sources 81–82 (1999) 891–895.
[13] M. Nakagawa, Master's Thesis, Kyushu University, Japan, (2004).
[14] M. Holzapfel, C. Jost, A. Prodi-Schwab, F. Krumeich, A. Würsig, H. Buqa, P. Novák, Carbon 43 (2005) 1488–1498.
[15] B. Garcia, S. Lavallée, G. Perron, C. Michot, M. Armand, Electrochim. Acta 49 (2004) 4583–4588.
[16] J. Fuller, R.T. Carlin, R.A. Osteryoung, J. Electrochem. Soc. 144 (1997) 3881–3885.
[17] B.J. Piersma, D.M. Ryan, E.R. Schumacher, T.L. Riechel, J. Electrochem. Soc. 143 (1996) 908–913.
[18] Y. Katayama, M. Yukumoto, T. Mimura, Electrochem. Solid-State Lett. 6 (2003) A96–A97.

[19] M. Egashira, T. Kiyabu, I. Watanabe, S. Okada, J. Yamaki, Electrochemistry 71 (2003) 1114–1116.
[20] M. Egashira, H. Todo, N. Yoshimoto, M. Morita, J. Yamaki, International meeting on lithium batteries, June 18–23, Biarritz, France, no. 426, 2006.
[21] T. Yoshimatsu, J. Hirai, Yamaki, J. Electrochem. Soc. 135 (1988) 2422–2427.
[22] M. Andersson, M. Herstedt, A.G. Bishop, K. Edström, Electrochim. Acta 47 (2002) 1885–1898.
[23] K. Endo, T. Tatsumi, J. Appl. Phys. 78 (1995) 1370–1372.
[24] D. Aurbach, A. Zaban, Y. Ein-Eli, I. Weissman, O. Chusid, B. Markovsky, M. Levi, E. Levi, A. Schechter, E. Granot, J. Power Sources 68 (1997) 91–98.